Real-time imaging reveals that noninvasive mammary epithelial acini can contain motile cells

Gray W. Pearson and Tony Hunter

Molecular and Cell Biology Laboratory, Salk Institute, La Jolla, CA 92037

To determine how extracellular signal–regulated kinases (ERK) 1/2 promote mammary tumorigenesis, we examined the real-time behavior of cells in an organotypic culture of the mammary glandular epithelium. Inducible activation of ERK1/2 in mature acini elicits cell motility and disrupts epithelial architecture in a manner that is reminiscent of ductal carcinoma in situ; however, motile cells do not invade through the basement membrane and branching morphogenesis does not take place. ERK1/2-induced motility causes cells to move both within the cell monolayer that contacts the basement membrane surrounding the acinus and through the luminal space of the acinus. E-cadherin expression is reduced after ERK1/2 activation, but motility does not involve an epithelial–mesenchymal transition. Cell motility and the disruption of epithelial architecture require a Rho kinase– and myosin light chain kinase–dependent increase in the phosphorylation of myosin light chain 2. Our results identify a new mechanism for the disruption of architecture in epithelial acini and suggest that ERK1/2 can promote noninvasive motility in preinvasive mammary tumors.

Introduction

The architecture of mammary glandular epithelium is disrupted during the development of preinvasive mammary lesions, such as ductal carcinoma in situ (DCIS). Interestingly, the gene expression profiling of DCIS lesions indicates that gene products that are not known to regulate proliferation or survival are also involved in tumor progression (Adeyinka et al., 2002; Ma et al., 2003; Porter et al., 2003). This suggests that the current mechanistic understanding of preinvasive epithelial tumor growth as being the product of excessive proliferation and resistance to cell death is incomplete and that there are additional unidentified cellular traits acquired during the preinvasive stage of tumor growth (Porter et al., 2003). A more precise understanding of mechanisms that promote the disruption of architecture that is observed in preinvasive tumors could assist in diagnosis and treatment of human breast cancer (Burstein et al., 2004).

The MAPK extracellular signal–regulated kinases (ERK) 1/2 are activated by receptor tyrosine kinases that promote the development of mammary tumors, and ERK1/2 are hyperactivated in breast cancer patient samples (Sivaraman et al., 1997; Mueller et al., 2000; Oh et al., 2001; Pearson et al., 2001). ERK1/2 are components of the Raf–MAPK/ERK kinase (MEK) 1/2–ERK1/2 MAPK module, which is a three-tiered kinase cascade that interprets physiological and pathological signaling cues to coordinate cell behavior through the phosphorylation of enzymatic and nonenzymatic substrates (Pearson et al., 2001). Because the Raf-MEK1/2-ERK1/2 MAPK module is a target of receptor tyrosine kinases amplified or overexpressed in breast cancer and hormones whose expression is elevated in the primary tumor microenvironment (Pearson et al., 2001), the regulation of cell behavior by ERK1/2 could be important in the phenotypes of mammary epithelial cells in a range of growth contexts. Therefore, determining how ERK1/2 regulates mammary epithelial cell behavior is critical to understanding mammary tumorigenesis.

To study epithelial cell behaviors during both organogenesis and tumorigenesis, researchers have used three-dimensional culture models that reconstitute the form and function of the tissue of interest (Schmeichel and Bissell, 2003). In one of these models, individual mammary epithelial cells plated on a reconstituted basement membrane (Matrigel) formed hollow polarized growth-arrested spheres of cells, termed acini (Debnath et al., 2003). The analysis of cell behavior during the formation of these model tissue structures has assisted in deciphering the mechanisms of tubule formation and how proliferation and apoptosis are balanced to form glandular architecture and maintain

Correspondence to Tony Hunter: hunter@salk.edu

Abbreviations used in this paper: 4-HT, 4-hydroxytamoxifen; DCIS, ductal carcinoma in situ; EMT, epithelial–mesenchymal transition; ERK, extracellular signal–regulated kinase; FMI, final mean intensity; HPV, human papillomavirus; MEK, MAPK/ERK kinase; MLC, myosin light chain; MLCK, MLC kinase; ROCK, Rho kinase.

The online version of this paper contains supplemental material.

The Journal of Cell Biology, Vol. 179, No. 7, December 31, 2007 1555–1567
http://www.jcb.org/cgi/doi/10.1083/jcb.200706099

tissue homeostasis in mammals (Debnath and Brugge, 2005). Furthermore, because epithelial tumors originate in the luminal epithelia that form ducts and lobules, organotypic culture models have also been instrumental in uncovering biochemical mechanisms and cell biological behaviors believed to be responsible for the early stages of mammary tumor development (Bissell and Radisky, 2001; Debnath and Brugge, 2005).

To identify mammary epithelial cell behaviors that are regulated by ERK1/2, we used real-time imaging as an unbiased discovery platform. Because organotypic culture models have successfully identified the underpinnings of preinvasive tumor growth, the cell behaviors discovered using real-time imaging could reflect the behavior of cells promoted by ERK1/2 in some cases of DCIS. Surprisingly, we have discovered that cells in polarized MCF-10A mammary epithelial acini become motile, but not invasive, through the basement membrane after persistent activation of the ERK1/2 MAPK pathway. This result was unexpected because the disrupted architecture of acini was previously believed to be exclusively promoted by increased cell proliferation, enhanced cell survival signaling, and the loss of cell polarity (Debnath and Brugge, 2005). This noninvasive motility was manifested as two previously unrecognized modes of ERK1/2-regulated cell motility, underpinned by the activation of the core cell actomyosin motility machinery, and did not require an epithelial–mesenchymal transition (EMT). The motility of cells was sustained for hours and the acini had an altered architecture reminiscent of DCIS, which suggests that, in principle, cells can become motile during the preinvasive stage of epithelial tumor growth.

Results

Real-time imaging reveals that ERK1/2 activation induces noninvasive forms of cell motility in epithelial acini

To specifically activate the Raf-MEK1/2-ERK1/2 MAPK module, we stably expressed a Raf-ER fusion protein in MCF-10A mammary epithelial cells. The Raf-ER protein consists of a constitutively active mutant of the Raf-1 kinase domain with the ligand-binding domain of the estrogen receptor fused to the C terminus (McMahon, 2001). The addition of estrogen or estrogen receptor antagonists, such as 4-hydroxytamoxifen (4-HT), promotes Hsp90 dissociation, which leads to a conformational change that increases Raf-ER protein stability and activation of MEK1/2 and ERK1/2 (McMahon, 2001). Treatment of Raf-ER–MCF-10A cells with 100 nM 4-HT was sufficient to activate ERK1/2 in monolayer culture and in cultured epithelial acini (unpublished data; see Noninvasive motility requires...). To achieve single-cell resolution, a GFP-histone fusion protein, H2B-GFP, was stably expressed in the Raf-ER–inducible MCF-10A mammary epithelial cells. This allowed us to track the positions of cells by following the nuclei, and by extension individual cells, using confocal microscopy. We imaged control acini treated with diluent and acini treated with 4-HT to activate Raf-ER at 30-min intervals over a 20.5-h period beginning 20 h after Raf-ER activation. In control acini, cells did not divide or change position (Fig. 1, A and B; and Video 1, available at http://www.jcb.org/cgi/content/full/jcb.200706099/DC1). In acini expressing activated Raf-ER, cells changed position in the x, y, and z planes (Fig. 1, A and B; and Video 2). This was a surprising result because previous work has claimed that only invasive cells are motile in organotypic culture models in vivo and similar to ours (Seton-Rogers et al., 2004). Treatment of MCF-10A cells expressing only H2B-GFP with 100 nM 4-HT did not have any detectable effect on cell behavior (unpublished data).

The ability of cells to move into the lumen, through the center of the acinus, and exit on the other side indicates that individual cells can insert themselves between other cells, a form of motility called intercalation, which is observed in *Drosophila melanogaster* epithelia during germ band extension (Irvine and Wieschaus, 1994; Munro and Odell, 2002; Schock and Perrimon, 2002). Cells changed interacting partners (Fig. 1 A, blue- and green-circled cells; and Video 3, available at http://www.jcb.org/cgi/content/full/jcb.200706099/DC1) and moved in opposing directions (Fig. 1 B, blue- and green-circled cells and total movement; and Video 4), which further demonstrates that cells are not moving as a collective unit or sheet, such as occurs during wound healing (Friedl and Wolf, 2003; Schneider and Haugh, 2006). We did not observe cells detach from the surface of the acinar structure, which is surrounded by a basement membrane, nor was there invasive growth of cell cords, which is often present in invasive ductal carcinomas. This finding is consistent with our results using phase-contrast imaging and our observation that acini containing activated Raf-ER maintained an intact laminin-rich basement membrane (Fig. 2 B). Raf-ER induction in MDCK cysts induces the formation of invasive tubules; however, these experiments were performed in cells grown in collagen and not in Matrigel (O'Brien et al., 2004). Thus, the differential response to Raf-ER induction could be influenced by both cell type and growth context. The failure of cells to penetrate the surrounding basement membrane is not a limitation of the assay because MDA-MB-231 cells form invasive structures under similar conditions (Park et al., 2006). To distinguish between motility associated with invasive growth through the basement membrane and the motility observed in Raf-ER–expressing acini, we will describe the observed cell behaviors collectively as noninvasive motility.

Individual cells had different motility rates, as indicated by the differences in the distance cells moved (Fig. 1 A, movement between intervals; and Video 2). The maximum rate of movement recorded was 360 nm/min. Cells did not necessarily achieve their highest speeds over the same time intervals (Fig. 1 B, total movement; and Video 4). This demonstrates that there is not a burst of movement that is propagated across all cells and indicates that cells are not moving as a sheet or unit. Cells did not sustain rates of over 300 nm/min for more than 1 h. Instead, cells accelerated to a maximum speed and then slowed down or stopped over subsequent time intervals (Fig. 1 B, 4-HT–treated blue-circled cell and total movement; and Video 4). The same cell could also begin accelerating again (Fig. 1 B, 4-HT–treated green-circled cell and total movement; and Video 4). Some cells showed no motility over the time frame of the experiment (Fig. 1 B, red-circled cell and total movement; and Video 4).

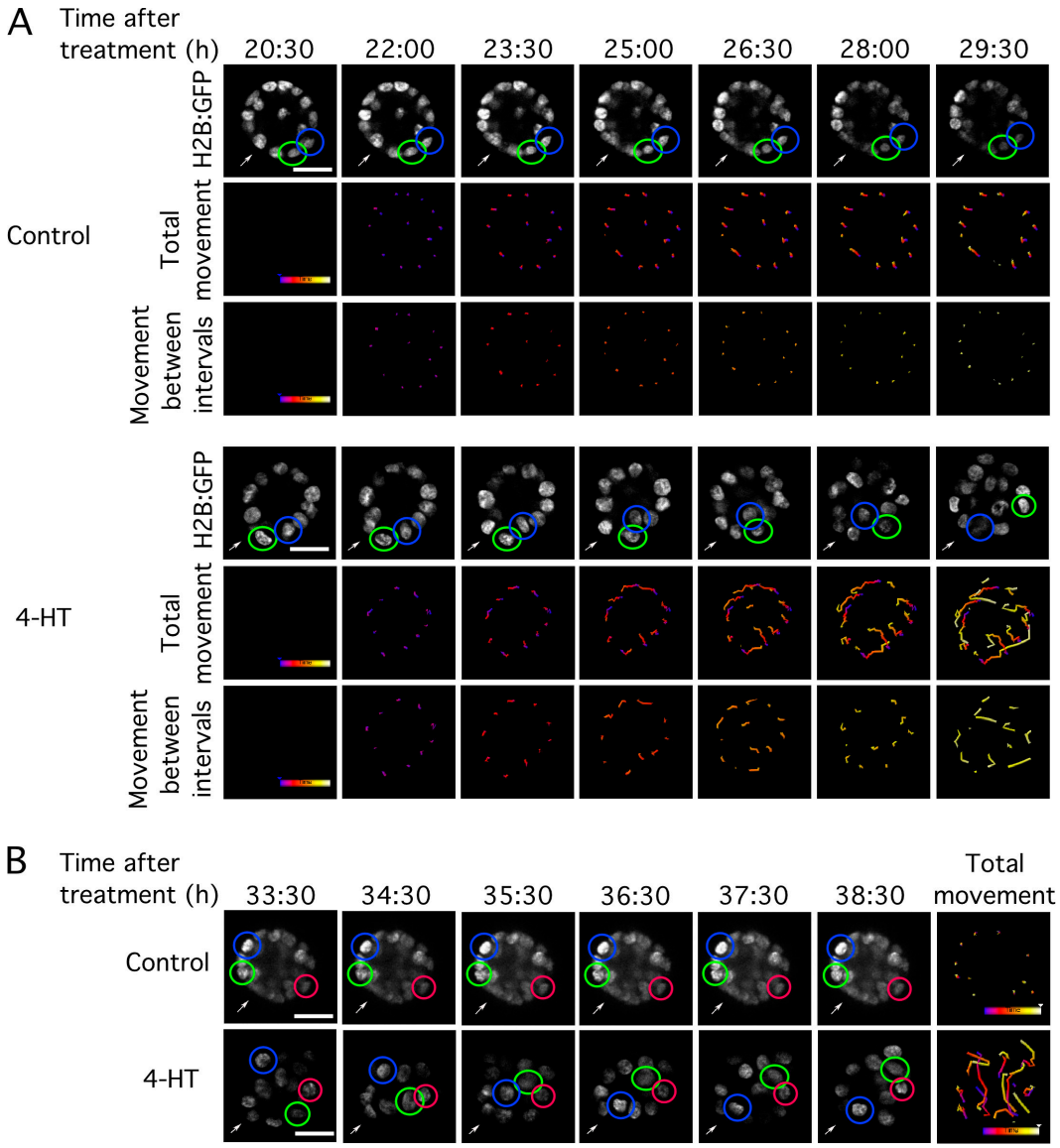

Figure 1. **Cells become motile but not invasive during the preinvasive disruption of epithelial acinar architecture.** (A) Day 10 Raf-ER–H2B-GFP–MCF-10A acini were treated with diluent or 100 nM 4-HT in culture media lacking EGF. After 20 h of treatment, acini were imaged at 30-min intervals for 20 h total by confocal microscopy (Videos 1 and 2, available at http://www.jcb.org/cgi/content/full/jcb.200706099/DC1). The top rows show equatorial confocal cross sections displaying H2B-GFP, which represents the nucleus, at 90-min intervals. The blue and green circles highlight the position of individual cells over time (Video 3). The arrow is added as a fixed reference point. Bars, 30 μm. The middle rows show the total movement of cells from the start of imaging. When cells depart the plane of view the cell track is removed. The bottom rows show the movement of cells over each 90-min interval. The colored scale bar represents increased time. (B) The same acinus shown in A is shown 13.5 h after the start of imaging. Displayed are 1-h intervals over 5 h. The red, blue, and green circles track the movement and motility characteristics of individual cells over time (Video 4). The red-circled cell does not move. The blue- and green-circled cells move in opposing directions and with different temporal regulation. The cells identified are not the same cells identified in B. Bar, 30 μM. The total movement of cells observed over the 5-h time interval is also shown. The colored scale bar represents increased time. The acini displayed in A and B are representative of at least 15 independent experiments.

Interestingly, motile cells displayed two new forms of ERK1/2-stimulated cell movement. We found that cells within an acinar structure can move around the surface of acini under the basement membrane (Fig. 1 A, 4-HT–treated green-circled cell; and Videos 2 and 3) and within the luminal space (Fig. 1, A [4-HT–treated blue-circled cell] and B [4-HT–treated green- and blue-circled cells]; and Videos 2–4). This indicates that cells in the surface monolayer of an acinus can intercalate between adjacent cells or between these cells and the basement membrane. To confirm these observations, we generated three-dimensional reconstructions of control and 4-HT–induced acini. Neither the cells on the surface nor cells in the lumen were motile in control acini (Fig. 2, A [1 and 2] and B; and Video 5, available at http://www.jcb.org/cgi/content/full/jcb.200706099/DC1). However, the three-dimensional reconstructions confirmed that in Raf-ER–stimulated acini, cells were moving around the surface of the acini (Fig. 2, A [1] and B; and Video 6) and within the lumen (Fig. 2, A [2 and 3] and B; and Video 6). The two types of movement are further demonstrated by the rotating the three-dimensional reconstructions of control and Raf-ER–induced acini on the z

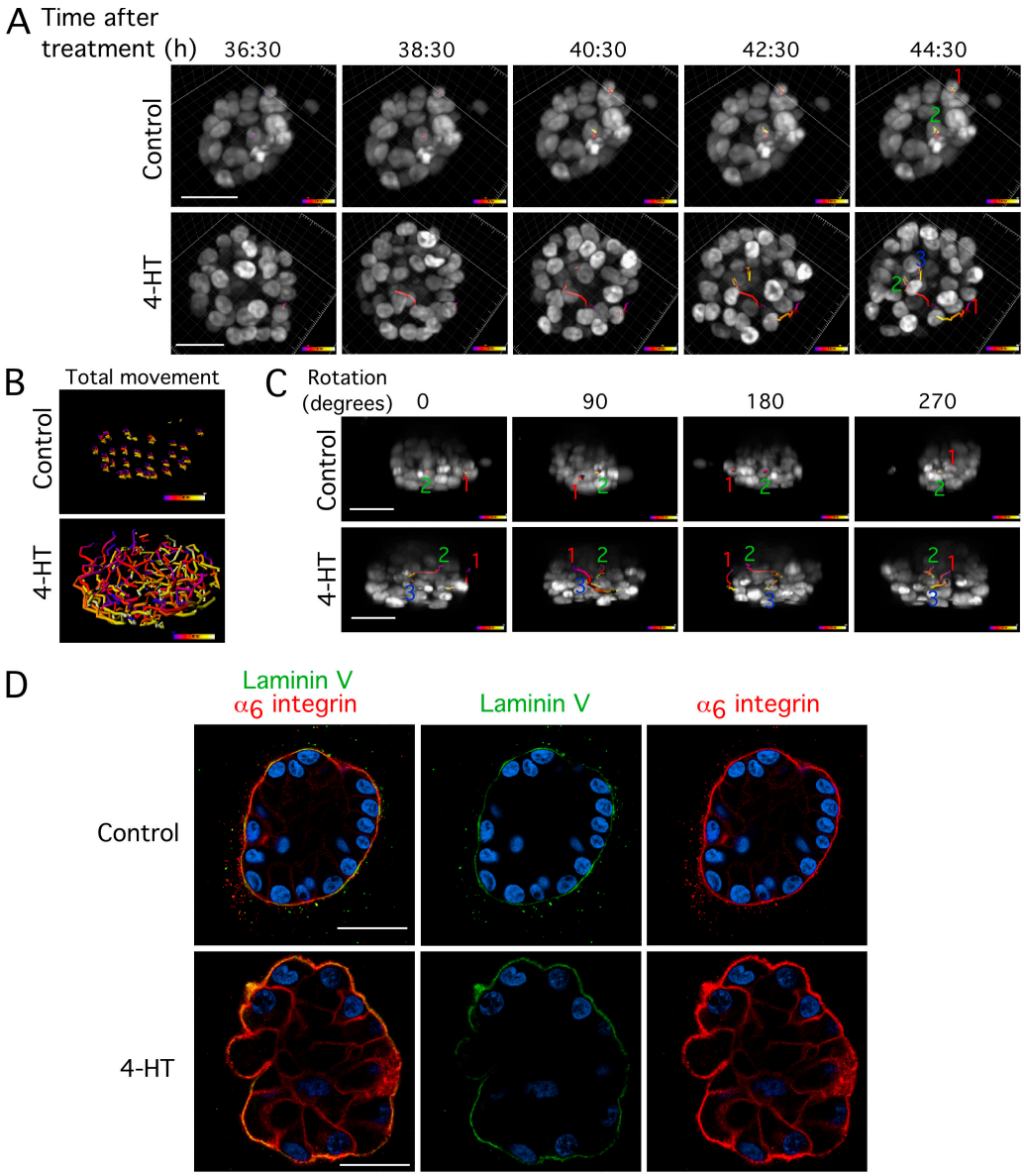

Figure 2. **Cells in contact with the ECM or surrounding epithelial cells are motile.** (A) Day 10 or later Raf-ER–H2B-GFP acini were treated with diluent or 100 nM 4-HT for 20 h and then imaged at 30-min intervals for at least 12 h. Shown are three-dimensional reconstructions of a 50-μm span of confocal images taken over time at 2-h intervals beginning 36.5 h after initial treatment. The acini are being viewed at a slight angle from the bottom up. The top level of cells in the acini is not visible in the reconstruction. The colored lines track the movement of selected cells on the outer surface (1) or the lumens (2 and 3) of the acini over the course of the experiment (Videos 5 and 6, available at http://www.jcb.org/cgi/content/full/jcb.200706099/DC1). The acini shown are representative of three independent experiments. Bars, 40 μm. Length of the side of a square in the grid, 10 μm. The colored tracks and scale bar represent increasing time. (B) The total cell movement from the acini in A is shown. (C) The acini from A at the 44.5-h time point are shown from the side with the bottom of the acini at the bottom of the panel and the identical numbered cell tracks. The acini are rotated on the z axis to demonstrate the location of cell movement within the acini (Videos 7 and 8). Bars, 40 μm. (D) Day 10 or later Raf-ER–H2B-GFP acini were treated with diluent or 100 nM 4-HT for 48 h. Acini were then fixed and immunostained with α–laminin V (green) and α–α_6 integrin (red) antibodies and counterstained with HOECHST (blue). The acini shown are representative of six independent experiments. Bars, 25 μm.

axis and observing the location of the cell tracks within the acini (Fig. 2 C and Videos 7 and 8). Cell track 1 for both the control and Raf-ER–induced acini is on the outer surface at either 0 or 180° of rotation (Fig. 2 C). Cell track 2 in the control acinus and cell track 3 in the Raf-ER–induced acinus never appear on the top, bottom, or side surfaces of the acini, which demonstrates that movement is entirely within the lumen (Fig. 2 C). Cell track 2 in the Raf-ER–induced acinus begins toward the surface and then extends into the interior of the acinus, which demonstrates that noninvasive cell movement can be directed away from the basement membrane (Fig. 2 C).

The two modes of movement we have demonstrated may use distinct molecular mechanisms to generate traction. The cells on the surface of acini are in contact with ECM proteins, such as laminin V (Fig. 2 D), and the basal surface of cells in contact with the ECM contains integrins (Fig. 2 D). Cells tracking along ECM proteins, such as the laminin found in the basement membrane on the basal surface of MCF-10A cells, use

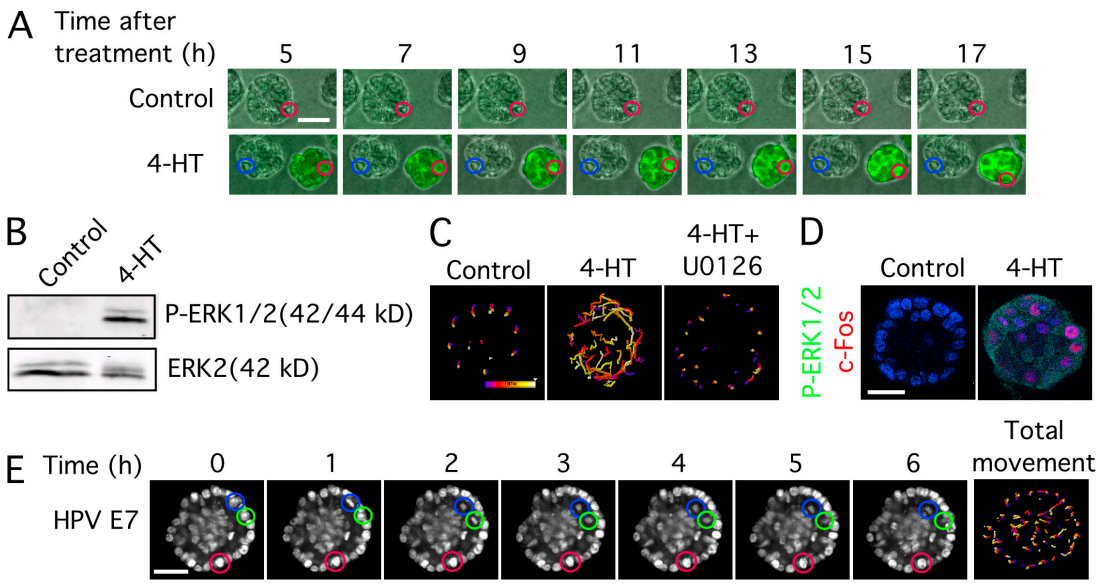

Figure 3. **Proliferation is not sufficient to induce noninvasive motility.** (A) Day 10 GFP–Raf-ER–MCF-10A acini were treated with diluent or 10 nM 4-HT for 5 h before imaging. Shown are phase contrast and GFP–Raf-ER at 2-h intervals over 12 h of imaging. The red and blue circles track the movement of individual cells over time. Bar, 30 μm. The acini shown are representative of five independent experiments. (B) Day 10 Raf-ER acini were treated with diluent or 100 nM 4-HT and grown for an additional 48 h. Lysates were immunoblotted with α–phospho-ERK1/2 (top) and α–ERK1/2 antibodies (bottom). (C) Day 10 Raf-ER–H2B-GFP acini were treated with diluent, 100 nM 4-HT, or 100 nM 4-HT and 10 μM U0126 (MEK1/2 inhibitor) simultaneously for 24 h and then imaged at 30-min intervals for 20 h total. Shown is the total movement of cells over the 20-h time period and is representative of eight independent experiments. The colored scale bar represents increased time. (D) Acini cultured, as described in B, were immunostained with α–phospho-ERK1/2 (green) and α–c-Fos (red) and counterstained with HOECHST (blue) to visualize the nuclei. Bar, 20 μM. (E) Day 10 HPV E7–H2B-GFP–MCF-10A acini were imaged at 1-h intervals over 18 h total. Shown are the H2B-GFP–labeled nuclei 5 h after imaging began at 1-h intervals over 6 h. The blue and green circles identify the daughter cells that have divided into the lumen. The red circle identifies a representative cell showing no motility. Bar, 30 μm. The total movement of cells over the 18 h of imaging is also shown. The acini in D and E are representative of three independent experiments.

integrin engagement with matrix proteins to supply traction (Hynes, 2002), so it is possible that cells on the surface of acini in organotypic culture also use integrins to supply traction. In contrast, epithelial cells tracking within the luminal space of acini are not in contact with the basement membrane. Instead, they are only in contact with epithelial cells that also reside in the luminal space and the apical surface of the epithelial cell monolayer that forms the surface of the acini (Fig. 2 D). Because integrins do not form contacts with adjacent cells, this suggests that when cells move within the lumen, they track along adjacent cells and therefore may use a distinct mechanism for traction. For example, when border cells migrate during *D. melanogaster* oogenesis, they use homophilic cadherin interactions to supply traction (Niewiadomska et al., 1999). However, we found that inhibitory antibodies directed toward β_1 integrin or E-cadherin did not influence noninvasive motility in our model (unpublished data). These results suggest that either blockade of additional adhesion molecules is necessary to stop noninvasive motility or that the basement membrane surrounding Raf-ER–induced acini reduces the effectiveness of these inhibitory antibodies.

Noninvasive motility requires acinus-autonomous ERK1/2 activation

To determine if the induction of noninvasive motility is directly related to Raf-ER expression, we used a GFP–Raf-ER fusion protein (Fig. 3 A). MCF-10A cells expressing a GFP–Raf-ER fusion protein were imaged 5 h after treatment with diluent or 10 nM 4-HT. As expected, GFP–Raf-ER–MCF-10A cells treated with diluent showed no change in appearance as judged by phase contrast (Fig. 3 A, top). The outline of individual cells can be seen (Fig. 3 A, red circles), which confirms that cells were not moving. GFP–Raf-ER acini treated with 10 nM 4-HT showed an increased GFP–Raf-ER signal intensity, which reflects an increase in stable expression level of the GFP–Raf-ER protein (Fig. 3 A, bottom; McMahon, 2001). As GFP–Raf-ER expression increased, cells began to move (Fig. 3 A). The acinus next to the GFP–Raf-ER–expressing acinus did not have a detectable level of GFP–Raf-ER expression and also did not display any change in appearance or cell motility as judged by phase contrast, which suggests that motility is acinus autonomous. All acini with detectable levels of GFP–Raf-ER had motile cells. Identical results were observed when GFP–Raf-ER–MCF-10A acini were treated with 100 nM 4-HT (unpublished data).

We also measured the movement of control and GFP–Raf-ER induced in sub-confluent cells grown in monolayer culture. Consistent with our results in organotypic culture, individual GFP–Raf-ER–induced cells are motile, whereas control cells are not (Videos 9 and 10, available at http://www.jcb.org/cgi/content/full/jcb.200706099/DC1). Although the expression level was modest, all motile cells contained detectable levels of GFP–Raf-ER. Also, the GFP–Raf-ER cells displayed variations in movement that were similar to what we observed in our organotypic culture model. Cells moved at different speeds and directions and in some cases were not motile at all.

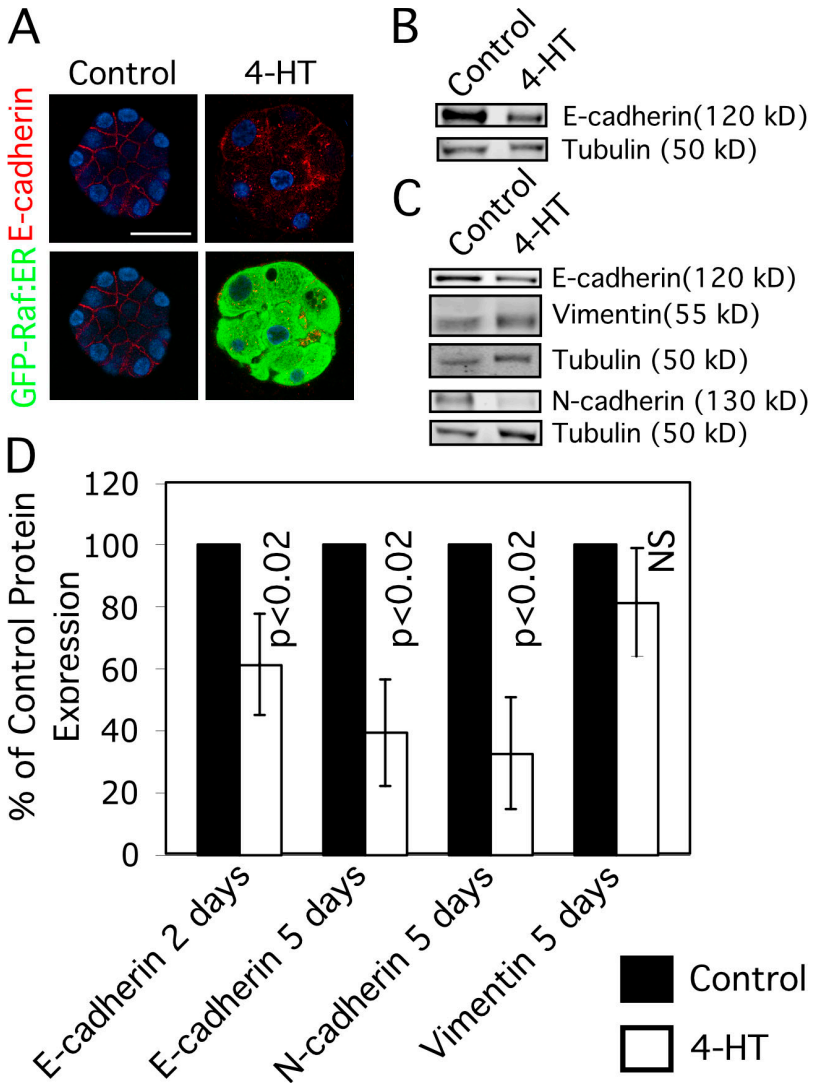

Figure 4. **Induction of noninvasive motility does not require EMT.** (A) Day 10 GFP–Raf-ER acini were treated with diluent or 100 nM 4-HT for 48 h, immunostained with α–E-cadherin antibody (red), and counterstained with HOECHST (blue). The top shows E-cadherin immunostaining and the bottom shows the expression level of GFP–Raf-ER. Bar, 25 μM. (B) Lysates from acini cultured as described in A were immunoblotted with α–E-cadherin and α–α-tubulin antibodies. The results are representative of at least three independent experiments. (C) Day 10 Raf-ER–H2B-GFP acini were treated with diluent or 100 nM 4-HT for 5 d. Lysates were immunoblotted with α–E-cadherin, α-vimentin, α–α-tubulin, or N-cadherin and α–α-tubulin antibodies, as described in Materials and methods, and are representative of four independent experiments. (D) The mean normalized expression level of the indicated protein in acini treated with 100 nM 4-HT (open bar) compared with control acini (shaded bar) is shown. The signal intensities for each protein were normalized to the expression of α-tubulin from the same lysate. The expression of the protein in the control acini was set at 100%. The error bars indicate the standard deviation. The statistical significance was judged by *t* test with $P > 0.05$ considered NS.

To ensure that the effects of Raf-ER activation were mediated by ERK1/2, we examined their phosphorylation state with an antibody that recognizes the dually phosphorylated activated form of ERK1/2. By immunoblotting, we found that ERK1/2 was activated in acini treated with 4-HT and that the level of phosphorylation correlated with expression level of the Raf-ER protein (Fig. 3 B; unpublished data). Activation of ERK1/2 was detected within 2 h of 4-HT treatment and peaked 24 h after treatment, which is similar to what has been previously observed in MCF-10A cells expressing Raf-ER grown as a monolayer (Schulze et al., 2001; unpublished data). Treatment with the pharmacological MEK1/2 inhibitor U0126 at the time of Raf-ER activation blocked induction of noninvasive motility (Fig. 3 C and Fig. S1, available at http://www.jcb.org/cgi/content/full/jcb.200706099/DC1), demonstrating that ERK1/2 activity is required. Raf-ER or GFP–Raf-ER expression was typically increased in at least 90% of cells within an individual acinar structure 48 h after administration of 4-HT (Fig. 3 A; unpublished data) and was reflected by increased phosphorylation of ERK1/2 and the expression of c-Fos, an indirect target of ERK1/2 signaling, in at least 90% of cells in acini (Fig. 3 D). The stochastic pattern of cell motility is therefore not likely to be caused by variations in Raf-ER expression or activity or downstream ERK1/2 activation.

Hyperproliferation is not sufficient to promote noninvasive motility

The Raf-MEK-ERK MAP kinase module stimulates proliferation in a range of contexts, including our organotypic culture model (Video 2). To determine whether hyperproliferation is sufficient to induce noninvasive motility, we observed human papillomavirus (HPV) E7–H2B-GFP acini in real time. The HPV E7 oncoprotein binds to and sequesters Rb, causing excessive proliferation of cells and increased acinar size; however, spherical architecture is maintained and cells in the luminal space undergo apoptosis (Debnath et al., 2002). In HPV E7, acini cell division was readily observed and most frequently oriented into the lumen; however, no cell motility was detected (Fig. 3 E, blue-, green-, and red-circled cells and total movement). These results demonstrate that the induction of noninvasive motility we observed is a product of ERK1/2 activation and not a secondary effect resulting from cell proliferation.

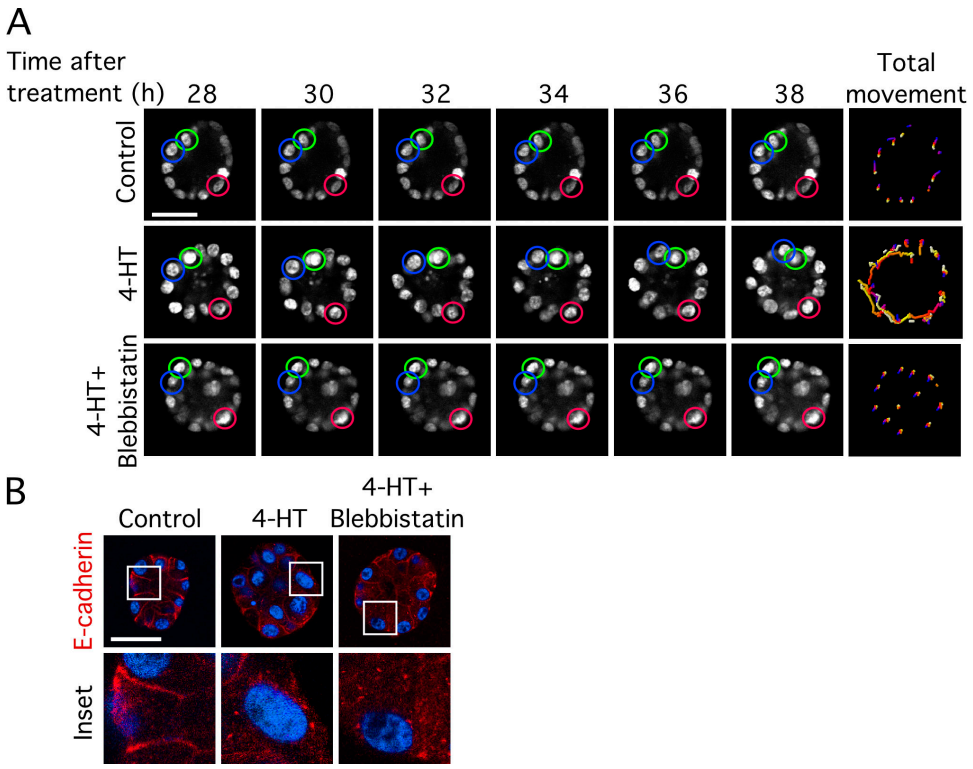

Figure 5. **Myosin contraction is necessary for noninvasive motility.** (A) Day 10 Raf-ER–H2B-GFP acini were treated with diluent, 100 nM 4-HT, or 100 nM 4-HT plus 25 μM blebbistatin for 24 h and then imaged for 16 h every 30 min. Shown are equatorial cross sections of H2B-GFP–labeled nuclei at 2-h intervals. The red, blue, and green circles identify individual cells over the time frame displayed. Bar, 25 μm. The total movement of cells over the course of 16 h of imaging is also shown. The acini displayed are representative of five independent experiments. (B) Raf-ER–H2B-GFP acini were cultured as described in A, immunostained with α–E-cadherin (red), and counterstained with HOECHST (blue). The area within the white squares in the top row is shown immediately below in the bottom row. The acini shown are representative of at least four independent experiments. Bar, 30 μm.

Induction of noninvasive motility does not require EMT

Carcinoma cells can exploit a preexisting biological program called the EMT, which promotes epithelial cell migration during development and wound healing. The induction of EMT is sufficient to induce invasive growth when MCF-10A cells are grown in organotypic culture (Irie et al., 2005). Because Raf-ER activation is sufficient to promote EMT in MDCK cells (Lehmann et al., 2000), we examined whether EMT occurred during the induction of noninvasive motility. Decreased E-cadherin expression is characteristic of EMT, and we found that E-cadherin expression was reduced at cell–cell junctions in GFP–Raf-ER–induced acini (Fig. 4 A). Examination of total E-cadherin expression by immunoblotting showed that the loss of E-cadherin at adhesion junctions is in part the result of reduced E-cadherin expression (Fig. 4, B and D). The expression level of N-cadherin (Thiery, 2002) is increased in cells that have undergone EMT (Grunert et al., 2003). When we examined acini 5 d after Raf-ER activation, which is sufficient to promote EMT in MDCK cells, we found, however, not only that N-cadherin expression was decreased but also that vimentin expression, another characteristic of cells that have undergone EMT, was unchanged or reduced (Fig. 4, C and D). Collectively, these results indicated that induction of noninvasive motility was not the result of cells undergoing EMT. We therefore next explored the molecular phenotypes that define the changes in epithelial character that promote noninvasive motility.

Myosin contraction is necessary for noninvasive motility in epithelial acini

Because EMT was not required for the induction of noninvasive motility, we had to establish a new set of molecular parameters for the induction of motility in epithelial acini. Myosin contraction is necessary for elongated, amoeboid, and intercalative motility and therefore was likely to be necessary for the various forms of noninvasive motility observed in acini expressing activated Raf-ER (Schock and Perrimon, 2002; Sahai and Marshall, 2003). At the time of Raf-ER activation, we treated acini with blebbistatin, a specific inhibitor of myosin II ATPase activity (Straight et al., 2003), in an attempt to specifically block induction of motility. When acini were treated with blebbistatin at the time of Raf-ER activation, cells did not become motile and disruption of epithelial architecture did not occur (Fig. 5 A). Similarly, addition of blebbistatin 48 h after Raf-ER was activated and cells had become motile was sufficient to block existing cell movement (unpublished data). Myosin contraction is necessary for disruption of cell–cell adhesion in some systems (Sahai and Marshall, 2002); however, we found that the relocalization of E-cadherin, which took place as a result of Raf-ER activation, did not require myosin contraction (Fig. 5 B). These results demonstrate an integral role for myosin contraction in the induction of motility in mammary epithelial acini. Furthermore, because blebbistatin treatment did not restore E-cadherin–based cell–cell adhesion, our data suggest that reduced cell

adhesion may be necessary, but is not sufficient for noninvasive cell movement.

Phosphorylation of myosin light chain (MLC) 2 is a biomarker of motility in epithelial acini

Because activation of Raf-ER caused a loss of E-cadherin expression at sites of cell adhesion, it was possible that cells in mammary epithelial acini have a constant propensity to move that is restrained by the establishment of cell–cell adhesion. Alternatively, the induction of noninvasive motility could require activation of motility-stimulating signaling pathways that lie dormant in mature acini. Myosin contraction is regulated by MLC2, which enhances the ATPase activity of myosin when phosphorylated at threonine 18 and/or serine 19 (Friedl and Wolf, 2003). Furthermore, phosphorylation of MLC2 on these sites is necessary for the motility of several cancer cell lines (Sahai and Marshall, 2003). To determine whether there is change in the cell motility regulatory program of cells with noninvasive motility, we examined the phosphorylation state of MLC2 by immunostaining with an MLC2 Ser-19 phosphospecific antibody. We found that there was an increase in phospho-MLC2^{S19} in acini expressing activated Raf-ER, but not in control acini or acini overexpressing HPV E7 (Fig. 6 A). The specificity of the antibody used to detect phospho-MLC2^{S19} was confirmed using a second independent phospho-MLC2^{S19}–specific antibody (Fig. S2, available at http://www.jcb.org/cgi/content/full/jcb.200706099/DC1). MLC2 phosphorylation was largely localized to the basal surface of cells in contact with the basement membrane, whereas the phospho-MLC2^{S19} detected in cells in the lumen did not show a polarized localization and they were not apoptotic (Figs. 6 B, 7 A, and S2). The localization of phospho-MLC2^{S19} therefore mimicked the localization of α_6 integrin (Fig. 2 B), which suggests that integrins, or other signaling complexes with a polarized localization, play a role in the local regulation of MLC2 phosphorylation.

We also examined the phosphorylation of MLC2 in GFP–Raf-ER–induced acini and found that the elevation of phospho-MLC2^{S19} was specific to GFP–Raf-ER–induced acini, which confirmed that the phosphorylation of MLC2^{S19} was directly linked to Raf-ER expression and ERK1/2 activation (Fig. 6 B). HPV E7 acini did contain detectable phospho-MLC2^{S19} in some luminal cells (Fig. 6 B); however, this is likely a consequence of Rho kinase (ROCK) 1 becoming cleaved by caspases in cells that are undergoing apoptosis (Coleman et al., 2001). To address whether the concentration of phospho-MLC2^{S19} we observed was caused by a redistribution of phospho-MLC2^{S19} or an increase in the total amount of phospho-MLC2^{S19}, we quantitated the total pixel intensity of phospho-MLC2^{S19} in control, HPV E7, and GFP–Raf-ER–induced acini. We found that there was a threefold increase in phospho-MLC2^{S19} pixel intensity within GFP–Raf-ER–induced acini compared with control (Fig. 6 C), whereas there was only a 1.3-fold increase in phospho-MLC2^{S19} pixel intensity within HPV E7 acini (not significant by *t* test). This suggests that there is an increase in the total amount of phospho-MLC2^{S19} within cells with noninvasive motility. Consistent with the increase in phospho-MLC2^{S19} pixel intensity we observed, induction of Raf-ER for 48 h in monolayer culture promoted a threefold increase in MLC2 phosphorylated on Thr-18 and Ser-19, as determined by immunoblotting with antibodies specific for dually phosphorylated MLC2 (Fig. 6 D). This result suggests that both Thr-18 and Ser-19 are phosphorylated in Raf-ER–induced acini.

MLC kinase (MLCK) and ROCK1/2 regulate MLC2 phosphorylation and noninvasive motility

The accumulation of Ser-19 phosphate on MLC2 is dependent on both direct phosphorylation by upstream kinases, such as MLCK, and on the inhibition of the myosin phosphatase complex mediated through ROCK1/2 phosphorylation (Sahai and Marshall, 2003). To investigate the signaling network responsible for regulating MLC2 phosphorylation in cultured acini, we treated cells with pharmacological inhibitors that target MLCK (ML-7) and ROCK1/2 (Y27632). MLCK directly phosphorylates MLC2 and is a substrate for ERK1/2 (Klemke et al., 1997), thus providing a direct link between the Raf-MEK1/2-ERK1/2 module and MLC2. ROCK1/2 not only phosphorylate MLC2, but also phosphorylate the myosin phosphatase–targeting subunit, thereby inhibiting myosin phosphatase (Friedl and Wolf, 2003). Raf-MEK1/2-ERK1/2 stimulation of ROCK1/2 is likely indirect, possibly through the increased production of autocrine growth factors (Schulze et al., 2001) that can activate Rho (Ridley and Hall, 1992). We treated acini with both ML-7 and Y27632 and immunostained for phospho-MLC2^{S19} to determine if MLCK and ROCK are required for MLC2 Ser-19 phosphorylation in epithelial acini (Fig. 7, A and B). When acini were treated with 4-HT, phospho-MLC2^{S19} was detected in 72% of acini, whereas only 5% of control acini contained phospho-MLC2^{S19} (Fig. 7 B). Treatment with ML-7 and Y27632 at the time of Raf-ER induction resulted in phospho-MLC2^{S19} being detected in just 12% of acini (Fig. 7 B). In addition, acini maintained a largely spherical architecture despite Raf-ER activation and c-Fos induction, an indicator of ERK1/2 activation (Fig. 7 A). Neither inhibitor alone reduced phospho-MLC2^{S19}, indicating that MLCK and ROCK1/2 can compensate for the loss of activity of the other kinase (unpublished data).

Pharmacological inhibitors of protein kinases often inhibit more than one kinase, so it is possible that ML-7 and Y27632 inhibition of kinases in addition to MLCK and ROCK1/2 was causal in blocking MLC2 phosphorylation. However, because c-Fos expression was unaffected by the inhibitors and because neither inhibitor alone had an effect, it is unlikely that the blockade of phospho-MLC2^{S19} is caused by severe nonspecific effects (Fig. 7 A). ROCK1/2 activity is necessary for disruption of E-cadherin adhesion in some cell types (Sahai and Marshall, 2002), but we did not observe any effect of combined treatment with ML-7 and Y27632 on E-cadherin relocalization in Raf-ER–expressing acini (Fig. 7 C). Collectively, our results indicate that in epithelial acini, ERK1/2 stimulates MLC2 phosphorylation through the coordinated activation of MLCK and ROCK1/2.

To determine whether the activities of MLCK and ROCK1/2 were required for induction of noninvasive motility, we next treated acini with ML-7 and Y27632 and quantitated the number

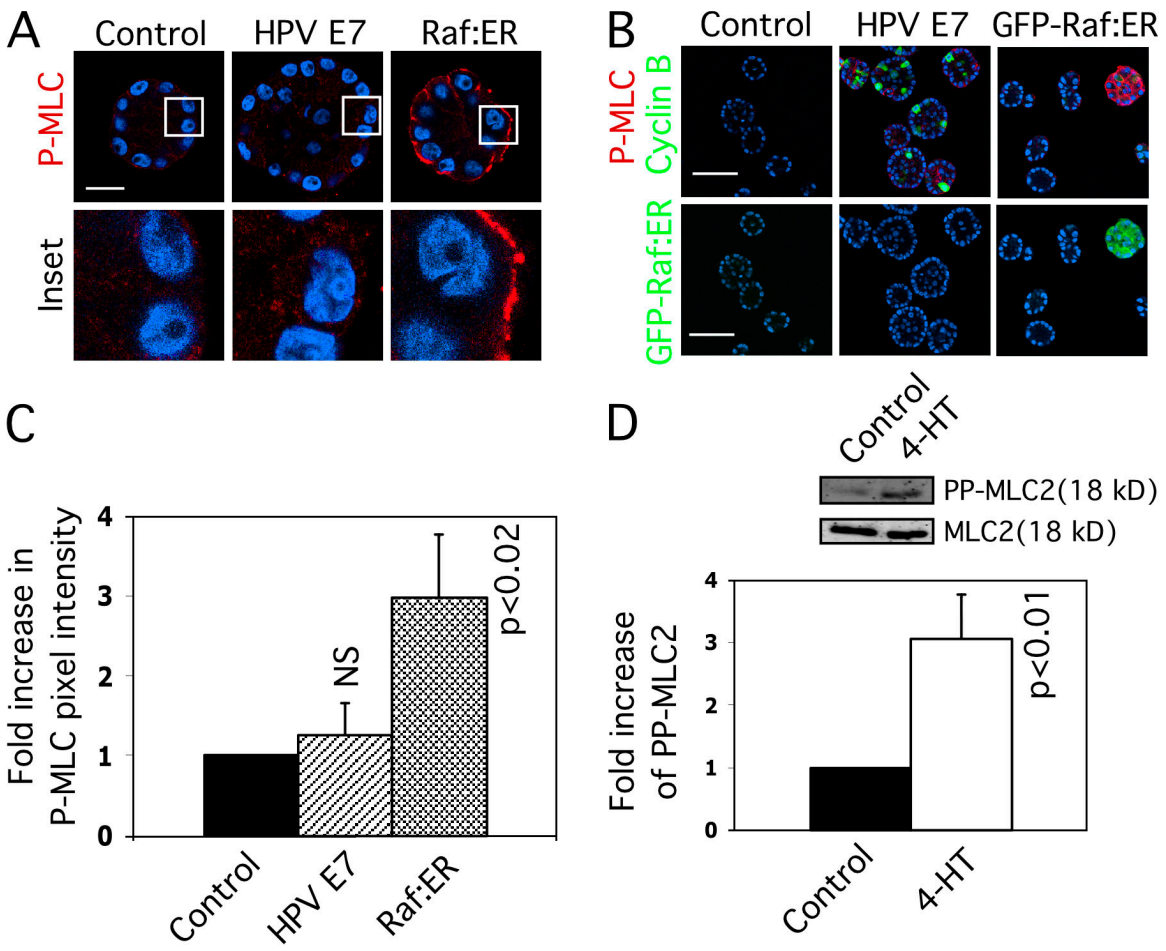

Figure 6. **MLC2 is phosphorylated in cells with noninvasive motility.** (A) Day 10 Raf-ER–H2B-GFP or HPV E7–H2B-GFP acini were treated with diluent or 100 nM 4-HT for 48 h, and then fixed and immunostained with α–phospho-MLC2^{S19} (red) and counterstained with HOECHST (blue). The area within the white square in the top row is shown immediately below. The acini shown are representative of three independent experiments. Bar, 25 μm. (B) Day 10 GFP–Raf-ER and HPV E7 acini were treated with diluent or 10 nM 4-HT for 48 h and then fixed and immunostained with α–phospho-MLC2^{S19} (red) and cyclin B (green) and counterstained with HOECHST (blue). The bottom panels show the level of GFP–Raf-ER expression in the acini depicted in the top panels. Bars, 75 μm. The acini shown are representative of four independent experiments. (C) The amount of phospho-MLC2^{S19} in at least 60 acini cultured as described in B was quantitated. The mean fold increase in α–phospho-MLC2^{S19} pixel intensity compared with control for three independent experiments is shown. The error bars represent the standard deviation. The statistical significance was judged by *t* test with $P > 0.05$ considered NS. (D) Raf-ER–H2B-GFP–MCF-10A cells were grown to confluence in monolayer culture and then cultured in organotypic culture Assay media lacking EGF with or without 100 nM 4-HT for 48 h. Lysates were immunoblotted with α–phospho-MLC2$^{T18/S19}$ or α-MLC2 antibodies. The mean fold increase for three independent experiments is shown. The error bar represents the standard deviation. The statistical significance was judged by *t* test with $P > 0.05$ considered NS.

of acini containing five or more motile cells. We never detected cell motility in all the control acini examined (Fig. 7, D and E; and Fig. S3, available at http://www.jcb.org/cgi/content/full/jcb.200706099/DC1). Activation of Raf-ER resulted in the induction of noninvasive motility in 55% of acini within 24 h (Fig. 7, D and E; and Fig. S2). Motility was only detected in 5% of acini when the acini were treated with inhibitors of MLCK and ROCK1/2 (Fig. 7, D and E; and Fig. S3). Treatment with either inhibitor alone had no effect on the induction of noninvasive motility, which is consistent with the failure of single agent treatment to block phospho-MLC2^{S19} (unpublished data). Consistent with MLC2 phosphorylation being required for noninvasive motility, treatment with blebbistatin reduced the number of acini with noninvasive motility to 4% but did not reduce MLC2 phosphorylation (Fig. 7, A, B, D, and E; and Fig. S3). These findings strongly suggest that the phosphorylation of MLC2 stimulated by MLCK and ROCK1/2 is an integral component of the biochemical signal transduction program that promotes noninvasive motility.

Discussion

The use of an organotypic culture model to study epithelial cell behavior has revealed that there are noninvasive forms of ERK1/2-induced cell movement. The discovery that epithelial cells can be motile in an organotypic culture model with features of DCIS suggests that cell motility develops before the detection of invasive growth in some fraction of human breast cancers and that this motility can promote the disruption of epithelial architecture. Movement of cells similar to that in our culture model can occur in vivo, as demonstrated by the observation that MTC nonmetastatic rat cells injected into the mammary fat pad can move relative to each other (Wang et al., 2002). Interestingly, because these cells were derived from an invasive primary tumor, the observation

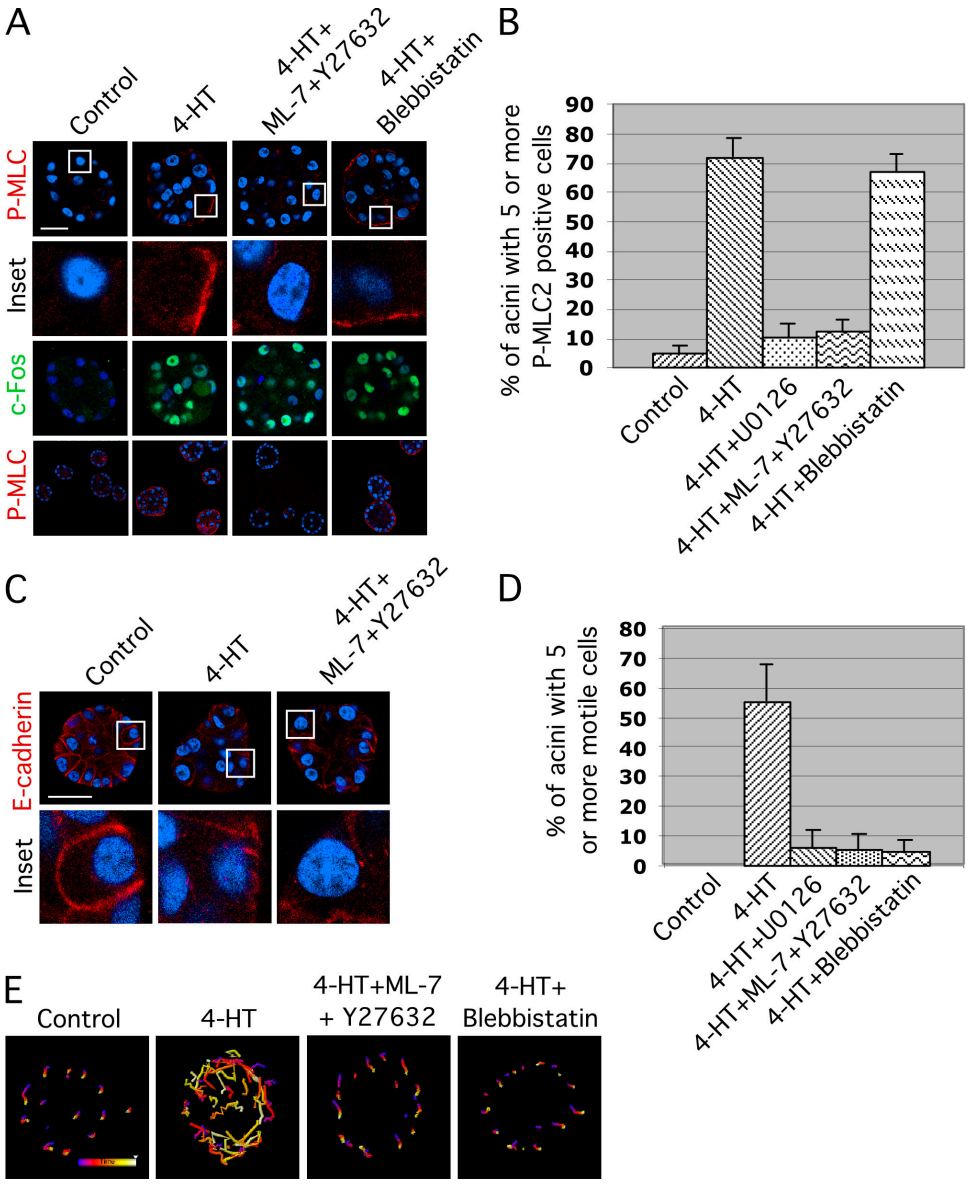

Figure 7. **MLCK and ROCK1/2 regulate the induction of noninvasive motility.** (A) Day 10 Raf-ER–H2B-GFP acini were treated with diluent, 100 nM 4-HT, or 100 nM 4-HT and indicated inhibitor, and then treated again 24 h later. 10 μM ML-7 and 40 μM Y27632 or 25 μM blebbistatin were used. 48 h after the first treatment, acini were fixed and immunostained with α–phospho-MLC^{S19} (red) and α–c-Fos (green) and counterstained with HOECHST (blue). The area within the white squares in the top row displaying the α–P-MLC^{S19} immunostaining is shown immediately below. The α–c-Fos immunostaining of the acini in the top row is shown in the row second from the bottom. Bar, 25 μm. (B) Acini were cultured as described in A and treated as indicated. 10 μM U0126 was used. The number of acini containing at least five MLC^{S19}-positive cells was scored. Shown is the mean ± SEM of 100 acini scored in three independent experiments. (C) Raf-ER–H2B-GFP acini were grown as treated as described in A with diluent, 100 nM 4-HT, or 100 nM 4-HT plus 10 μM ML-7 and 40 μM Y27632. After 48 h total treatment time, acini were fixed and immunostained with α–E-cadherin (red) and counterstained with HOECHST (blue). The area within the white squares is shown in the panels immediately below. Bar, 25 μm. (D) Raf-ER–H2B-GFP acini were cultured as described in A. After 24 h of initial treatment, fresh media with diluent, 4-HT, or 4-HT and inhibitor were added 1 h before confocal imaging at 30-min intervals for 20 h total. 10 μM U0126 was used. The number of acini containing five moving cells that changed their original position relative to the other cells in the acini was scored. Shown is the mean ± SEM of 10 acini scored in three independent experiments. All treatment conditions were assayed in an individual experiment. (E) Cells were cultured and imaged as described in D. The total movement of cells over the complete imaging is also shown. All treatment conditions were assayed in an individual experiment. The colored scale bar represents increased time.

that cells were motile was not considered notable. Because the parental MCF-10A cells in our model are not invasive, we can definitively conclude that the motility we observed is not a by-product of invasive growth and thus could be acquired during the preinvasive stage of tumor development.

The two modes of noninvasive motility observed in our organotypic culture model have also been observed during branching morphogenesis in salivary gland explants and the ureteric bud of the kidney (Shakya et al., 2005; Larsen et al., 2006). The motility in the salivary gland was halted after acinar development, which indicated this was an embryonic cell behavior (Larsen et al., 2006). We demonstrate that after formation of acini in mammary organotypic culture, dynamic cell movements can be initiated when there is persistent activation of the

Raf-MEK1/2-ERK1/2 MAPK module. Because branching morphogenesis was not the end product of the dynamic movements we observed, our results suggest that ERK1/2 can promote cell movements in epithelial lesions with a disrupted architecture, such as preinvasive epithelial cancers, by engaging a portion of the motility program used by epithelial cells during branching morphogenesis. Our results also suggest that ERK1/2 activation can promote noninvasive motility during embryonic development of the salivary gland and the kidney and possibly other epithelial tissues. Considering the fact that noninvasive epithelial cell movements contribute to the development of multiple epithelial tissues, such movements are likely to contribute to the development of the mammary gland in a manner regulated by ERK1/2. Interestingly, both developing MDCK and lung alveolar type II cell cysts grown on Matrigel appear to have noninvasive cell movements as judged by phase-contrast imaging (Yu et al., 2007), which supports the hypothesis that acini developing in organotypic culture recapitulate epithelial movements that occur during glandular morphogenesis. We are currently investigating the role of noninvasive motility in the morphogenesis of mammary epithelial acini in both our organotypic culture model and the in vivo development of mammary gland.

We have found that myosin contraction is necessary for the movement of cells in mammary epithelial acini, which demonstrates that contraction is a critical component of noninvasive motility. ERK1/2 regulate contraction by stimulating the phosphorylation of MLC2 through MLCK and ROCK1/2. MLCK is a known substrate for ERK1/2, thus providing a direct mechanism for activation (Klemke et al., 1997). In contrast, ROCK1/2 are not known to be ERK1/2 substrates and thus are likely activated through an indirect mechanism. One possibility is that ROCK1/2 are activated by autocrine growth factors because persistent ERK1/2 activation promotes the production of heparin-binding epidermal growth factor, amphiregulin, transforming growth factor α, vascular endothelial growth factor, and fibroblast growth factor 2 (McCarthy et al., 1995; Schulze et al., 2001). ERK1/2 could also induce ROCK1/2 through indirect intracellular cross talk, such as the ERK1/2-stimulated transcription of a protein or complement of proteins that stimulate the GTP loading of Rho. Interestingly, genetic ablation of Raf-1 in fibroblasts and keratinocytes causes the mislocalization and activation of ROCK2 (Ehrenreiter et al., 2005). Combined with our results, these findings suggest that the role of Raf-1 in the regulation of ROCK1/2 is cell type specific. It is also possible that Raf-1 suppresses, whereas B-Raf, through ERK1/2, promotes the activation of ROCK1/2. Also of note is the fact that pharmacological and genetic inhibition of MEK1/2 increases MLC2 phosphorylation in a ROCK1/2-dependent manner in endothelial cells (Mavria et al., 2006). Therefore, determining exactly how cell type and genetic context influence whether ERK1/2 activity promotes or reduces ROCK1/2 activity will be necessary to determine how to effectively use pharmacological inhibitors of the Raf-MEK1/2-ERK1/2 MAPK cascade.

Mammary epithelial cells are endowed with a plasticity that allows for the expansion of the mammary glandular epithelium during puberty and pregnancy. Our results demonstrate that there is a molecularly defined point within the range of epithelial plasticity where cell motility signaling pathways are activated and cell–cell adhesion is compromised. These molecular changes promote the movement of mammary epithelia along the surface and within the lumen of the mammary glandular epithelium in a manner dependent on actin-myosin contraction; however, this movement is not sufficient for invasion through the surrounding basement membrane. Whether epithelial cells with noninvasive motility require a reactive stroma or if further alterations to the tumor genome are necessary for tumors to become invasive is an area for future research that we are investigating.

Materials and methods

Cell culture and reagents

MCF-10A human mammary epithelial cells were obtained from American Type Culture Collection and were cultured in DME/F12 (Invitrogen) supplemented with 5% horse serum (Invitrogen), 10 μg/ml insulin (Research Diagnostics, Inc), 20 ng/ml epidermal growth factor (Research Diagnostics, Inc.), 500 ng/ml hydrocortisone (Sigma-Aldrich), 100 ng/ml cholera toxin (EMD), and ciprofloxacin (Cellgro). The growth factor–reduced Matrigel (BD Biosciences) used in these experiments had protein concentrations between 10 and 12 mg/ml. 4-HT, U0126, ML-7, Y27632, and blebbistatin were obtained from EMD. Antibodies used were c-Fos, vimentin, MLC2 (sc-28329 and sc-15370), and ERK2 (Santa Cruz Biotechnology, Inc.); α_6 integrin and laminin V (Chemicon); phosphorylated MLC2^{S19} (mouse), phosphorylated MLC2^{S19} (rabbit), phosphorylated MLC2$^{T18/S19}$ (Cell Signaling Technology); E- and N-cadherin (BD Biosciences); and phosphorylated ERK2(T183, Y185) and α-tubulin (Sigma-Aldrich). Secondary antibodies labeled with Alexa fluor 488, 568, 647, and 680 (Invitrogen) and IRDye800 (Rockland Immunochemicals) were used. HOECHST 33342 was obtained from EMD.

Retroviral vectors and cell lines

The vector pCLNRX–H2B-GFP was a gift from E.T. Wong and G. Wahl (Salk Institute, La Jolla, CA), pBABE–Raf-ER was gift from M. White and R. Bumeister (University of Texas Southwestern Medical Center, Dallas, TX), pBABE–GFP–Raf-ER was a gift from M. McMahon (University of California, San Francisco, San Francisco, CA), and pCLXSN-HPV E7 was a gift from D. Galloway (Fred Hutchinson Cancer Research Center, Seattle, WA). Vesicular stomatitis virus G–pseudotyped virus was generated by transfecting HEK293 cells that stably express Gag and Pol with vesicular stomatitis virus G and pBABE–Raf-ER, pBABE–GFP–Raf-ER, pCLNRX–H2B-GFP, or pCLXSN–HPV E7. Viral supernatant was collected 48–96 h after transfection, filtered through a 0.4-μm filter, and supplemented with 4 μg/ml polybrene (Sigma-Aldrich). 500,000 MCF-10A cells plated in a 10-cm plate were infected. Cells were cultured in 500 ng/ml puromycin or 400 μg/ml G418 to create stable pBABE–Raf-ER–MCF-10A or pCLXSN-HPV E7 cells. To create Raf-ER–H2B-GFP cells, stable pools of pBABE–Raf-ER–MCF-10A cells were infected with pCLNRX–H2B-GFP and selected with 400 μg/ml G418. To generate HPV E7–H2B-GFP cells, stable pools of pCLXSN–HPV E7–MCF-10A cells were infected with pCLNRX–H2B-GFP. Because the HPV E7–MCF-10A cells were already G418 resistant, we did not perform further drug selection. The infection rate with pCLNRX–H2B-GFP typically exceeds 80% of cells, therefore providing a sufficient population of acini for real-time imaging. We did not observe any difference in HPV E7 acini that expressed H2B-GFP and those that did not, as judged by acini diameter or staining for markers of proliferation or phospho-MLC2. The GFP–Raf-ER–MCF-10A cells were not selected to allow direct comparison of acini that expressed GFP–Raf-ER and those that did not.

Three-dimensional morphogenesis assay

MCF-10A cells were plated in 8-well chamberslides (Falcon) for immunofluorescence staining or 8-well chambered coverglass (Thermo Fisher Scientific) for real-time imaging. First, a solid layer of Matrigel was plated into the wells. Then, 5,000 cells resuspended in 2% Matrigel and Assay media (Phenol red–free DME/F12 supplemented with 2% horse serum, 10 μg/ml insulin, 1 ng/ml EGF, 500 ng/ml hydrocortisone, 100 ng/ml cholera toxin, and cyprofloxacin (Cellgro) were added to the plate. On days 4 and 8, the 2% Matrigel assay media mixture was replaced. On day 10, Raf-ER–H2B-GFP cultures were treated with a combination of vehicle, 100 nM 4-HT, or 100 nM 4-HT plus inhibitor in 2% Matrigel assay media mixture without EGF. GFP–Raf-ER acini were treated with 10 nM 4-HT. HPV E7–H2B-GFP cultures

were refreshed with assay media containing 1 ng/ml EGF on day 10 and before imaging. When inhibitors were used and for real-time imaging experiments, the media was refreshed within 24 h.

Immunoblot analysis

12,000–15,000 acini were lysed in RIPA buffer supplemented with protease and phosphatase inhibitors and protein levels normalized using Cyto-tox One (Promega) according to the manufacturer's instructions. Immunoblots were visualized using an infrared scanner (Odyssey; LI-COR). Quantitation of protein signal was performed using Odyssey software. For E-cadherin, N-cadherin, and vimentin quantitation, protein band intensity for each gel lane was normalized to the level of α-tubulin expression in the same lane. For phospho-MLC2$^{T18/S19}$ quantitation, the intensity of the phospho-MLC2$^{T18/S19}$ signal was divided by the intensity of the MLC2 signal to obtain a normalized phospho-MLC2$^{T18/S19}$ value. The normalized phospho-MLC2$^{T/18/S19}$ from the 4-HT–treated cells was divided by the normalized value from the control cells to determine the fold increase.

Immunofluorescence staining

Cultures were fixed in 2% formalin (Sigma-Aldrich) in PBS for 20 min, permeabilized with 0.5% Triton X-100 in PBS for 10 min at room temperature, immunostained as previously described (Debnath et al., 2003), and mounted using ProLong Gold antifade reagent (Invitrogen). All steps were performed at room temperature. Images were acquired using Leica software in TIFF format on a confocal microscope (SP2 AOBS; Leica) with either 20×/0.7 (HC PL APO lbd.BL; Leica) or 63×/1.4 (HCX PL APO lbd.BL; Leica) objectives. Images were arranged using Photoshop 7.0 (Adobe) and Canvas 8 (Deneba Systems). Quantitation of the fold increase in phospho-MLC2 pixel intensity was performed using Leica software. The mean pixel intensity for an individual acinus was obtained by drawing a region of interest around each acinus to obtain a mean intensity value for the each acinus. The mean pixel intensity for an equivalent region of interest in an area of Matrigel alone in the same field of view was then obtained and subtracted from the mean intensity of the acinus to obtain a final mean intensity (FMI) value for the acinus. The mean of the FMIs of at least 60 acini was then determined to obtain the mean FMI for each condition of the experiment. The mean FMI for the HPV E7 acini or GFP–Raf-ER acini was divided by the mean FMI of the control acini to determine the fold increase in phospho-MLC2 pixel intensity.

Real-time imaging

Three-dimensional cultures were grown in 8-well chambered coverglass with a #1.5 coverglass bottom (Thermo Fisher Scientific) as described in Three-dimensional morphogenesis assay. Media containing the indicated components was refreshed before imaging, and within 15 min the cultures were placed on the stage of an inverted microscope (DMIRE2; Leica) with a real-time confocal scanhead (QLC100 spinning disk confocal; Yokogawa) housed in a 37°C chamber enriched with humidified CO_2 (Solent). Images were acquired with a camera (C9100-02 EM–charge coupled device; Hamamatsu) using SimplePCI software (Compix) and a 40×/0.60 objective (HCX Plan Flour; Leica). In each experiment, at least six different x,y coordinates were selected for each growth condition. Typically, three z-axis positions were selected for each x,y coordinate. For three-dimensional reconstructions, z slices were taken at 1-μm intervals over a span of at least 70 μm. The acini selected were mostly spherical at the start of the experiment, allowing the transition from normal to disrupted architecture to be visualized. Use of the 8-well chamber slides allowed us to compare multiple treatment conditions in an individual experiment and therefore rule out the contribution of variations in the growth conditions at the time of image acquisition. For imaging of cells in monolayer culture, 5,000 cells per well were plated in 8-well chambered coverglass (Ibidi). 18 h after plating the cells, the culture media was switched to Assay media lacking EGF, supplemented with diluent or 100 nM 4-HT. 24 h after initial stimulation, media was refreshed and the subconfluent cells were imaged as described earlier in the paragraph for three-dimensional cultures, with the exception that a 20×/0.40 objective (N Plan L; Leica) was used. For static presentation, movies were exported as image files using Quicktime Pro software (Apple) and arranged in Photoshop 7.0 and Canvas 8. Cell movement was analyzed using Imaris software (Bitplane). For three-dimensional reconstructions, confocal slices in TIFF format acquired at 1-μm intervals were assembled by Imaris software. For image clarity and management of file size, the reconstructions were cropped to a depth of 50 μm in the z axis. The cells on the bottom of the acini in contact with the basement membrane are brighter than the acini on the top, because of decreased light penetration. The acquisition parameters and laser intensity were set to maintain a linear range of signal intensity.

Online supplemental material

Video 1 shows that cells in control acini are not motile. Video 2 shows that noninvasive motility promotes the disruption of epithelial architecture when ERK1/2 is persistently activated. Video 3 shows that cells can enter and exit the lumen but do not become invasive. Video 4 shows that cells can move at different speeds and in different directions. Video 5 shows a partial three-dimensional reconstruction of a control acinus and demonstrates that cells are not motile on the surface or the lumen. Video 6 shows a partial three-dimensional reconstruction that shows the movement of cells in a 4-HT–induced acinus. Video 7 is a partial three-dimensional reconstruction of a control acinus rotating on the z axis that shows that neither cells on the surface or in the lumen are motile. Video 8 is a partial three-dimensional reconstruction of a Raf-ER–induced acinus rotating on the z axis that shows that both cells on the surface and in the lumen are motile. Video 9 shows that uninduced GFP–Raf-ER cells in monolayer culture are not motile. Video 10 shows that 4-HT–induced GFP–Raf-ER cells in monolayer culture are motile. Fig. S1 shows time-lapse images demonstrating that MEK1/2 is necessary for induction of noninvasive motility. Fig. S2 shows costaining of control and 4-HT–stimulated acini with two different α–phospho-MLC2^{S19} antibodies. Fig. S3 shows time-lapse images demonstrating that MLCK and ROCK1/2 are necessary for induction of noninvasive motility. Online supplemental material is available at http://www.jcb.org/cgi/content/full/jcb.200706099/DC1.

We thank Gina Yanochko for useful discussions.

This work was supported by grant T32CA009370 (G.W. Pearson) and grants CA14195 and CA82683 (T. Hunter) from the National Cancer Institute. G.W. Pearson is a recipient of a Genentech Foundation Fellowship. T. Hunter is a Frank and Else Schilling American Cancer Society Research Professor.

The authors have no conflicting financial interests.

Submitted: 15 June 2007
Accepted: 25 November 2007

References

Adeyinka, A., E. Emberley, Y. Niu, L. Snell, L.C. Murphy, H. Sowter, C.C. Wykoff, A.L. Harris, and P.H. Watson. 2002. Analysis of gene expression in ductal carcinoma in situ of the breast. *Clin. Cancer Res.* 8:3788–3795.

Bissell, M.J., and D. Radisky. 2001. Putting tumours in context. *Nat. Rev. Cancer*. 1:46–54.

Burstein, H.J., K. Polyak, J.S. Wong, S.C. Lester, and C.M. Kaelin. 2004. Ductal carcinoma in situ of the breast. *N. Engl. J. Med.* 350:1430–1441.

Coleman, M.L., E.A. Sahai, M. Yeo, M. Bosch, A. Dewar, and M.F. Olson. 2001. Membrane blebbing during apoptosis results from caspase-mediated activation of ROCK I. *Nat. Cell Biol.* 3:339–345.

Debnath, J., and J.S. Brugge. 2005. Modelling glandular epithelial cancers in three-dimensional cultures. *Nat. Rev. Cancer*. 5:675–688.

Debnath, J., K.R. Mills, N.L. Collins, M.J. Reginato, S.K. Muthuswamy, and J.S. Brugge. 2002. The role of apoptosis in creating and maintaining luminal space within normal and oncogene-expressing mammary acini. *Cell*. 111:29–40.

Debnath, J., S.K. Muthuswamy, and J.S. Brugge. 2003. Morphogenesis and oncogenesis of MCF-10A mammary epithelial acini grown in three-dimensional basement membrane cultures. *Methods*. 30:256–268.

Ehrenreiter, K., D. Piazzolla, V. Velamoor, I. Sobczak, J.V. Small, J. Takeda, T. Leung, and M. Baccarini. 2005. Raf-1 regulates Rho signaling and cell migration. *J. Cell Biol.* 168:955–964.

Friedl, P., and K. Wolf. 2003. Tumour-cell invasion and migration: diversity and escape mechanisms. *Nat. Rev. Cancer*. 3:362–374.

Grunert, S., M. Jechlinger, and H. Beug. 2003. Diverse cellular and molecular mechanisms contribute to epithelial plasticity and metastasis. *Nat. Rev. Mol. Cell Biol.* 4:657–665.

Hynes, R.O. 2002. Integrins: bidirectional, allosteric signaling machines. *Cell*. 110:673–687.

Irie, H.Y., R.V. Pearline, D. Grueneberg, M. Hsia, P. Ravichandran, N. Kothari, S. Natesan, and J.S. Brugge. 2005. Distinct roles of Akt1 and Akt2 in regulating cell migration and epithelial–mesenchymal transition. *J. Cell Biol.* 171:1023–1034.

Irvine, K.D., and E. Wieschaus. 1994. Cell intercalation during *Drosophila* germband extension and its regulation by pair-rule segmentation genes. *Development*. 120:827–841.

Klemke, R.L., S. Cai, A.L. Giannini, P.J. Gallagher, P. de Lanerolle, and D.A. Cheresh. 1997. Regulation of cell motility by mitogen-activated protein kinase. *J. Cell Biol.* 137:481–492.

Larsen, M., C. Wei, and K.M. Yamada. 2006. Cell and fibronectin dynamics during branching morphogenesis. *J. Cell Sci.* 119:3376–3384.

Lehmann, K., E. Janda, C.E. Pierreux, M. Rytomaa, A. Schulze, M. McMahon, C.S. Hill, H. Beug, and J. Downward. 2000. Raf induces TGFβ production while blocking its apoptotic but not invasive responses: a mechanism leading to increased malignancy in epithelial cells. *Genes Dev.* 14:2610–2622.

Ma, X.J., R. Salunga, J.T. Tuggle, J. Gaudet, E. Enright, P. McQuary, T. Payette, M. Pistone, K. Stecker, B.M. Zhang, et al. 2003. Gene expression profiles of human breast cancer progression. *Proc. Natl. Acad. Sci. USA*. 100:5974–5979.

Mavria, G., Y. Vercoulen, M. Yeo, H. Paterson, M. Karasarides, R. Marais, D. Bird, and C.J. Marshall. 2006. ERK-MAPK signaling opposes Rho-kinase to promote endothelial cell survival and sprouting during angiogenesis. *Cancer Cell*. 9:33–44.

McCarthy, S.A., M.L. Samuels, C.A. Pritchard, J.A. Abraham, and M. McMahon. 1995. Rapid induction of heparin-binding epidermal growth factor/diphtheria toxin receptor expression by Raf and Ras oncogenes. *Genes Dev.* 9:1953–1964.

McMahon, M. 2001. Steroid receptor fusion proteins for conditional activation of Raf-MEK-ERK signaling pathway. *Methods Enzymol.* 332:401–417.

Mueller, H., N. Flury, S. Eppenberger-Castori, W. Kueng, F. David, and U. Eppenberger. 2000. Potential prognostic value of mitogen-activated protein kinase activity for disease-free survival of primary breast cancer patients. *Int. J. Cancer*. 89:384–388.

Munro, E.M., and G.M. Odell. 2002. Polarized basolateral cell motility underlies invagination and convergent extension of the ascidian notochord. *Development*. 129:13–24.

Niewiadomska, P., D. Godt, and U. Tepass. 1999. DE-Cadherin is required for intercellular motility during *Drosophila* oogenesis. *J. Cell Biol.* 144:533–547.

O'Brien, L.E., K. Tang, E.S. Kats, A. Schutz-Geschwender, J.H. Lipschutz, and K.E. Mostov. 2004. ERK and MMPs sequentially regulate distinct stages of epithelial tubule development. *Dev. Cell*. 7:21–32.

Oh, A.S., L.A. Lorant, J.N. Holloway, D.L. Miller, F.G. Kern, and D. El-Ashry. 2001. Hyperactivation of MAPK induces loss of ERα expression in breast cancer cells. *Mol. Endocrinol.* 15:1344–1359.

Park, C.C., H. Zhang, M. Pallavicini, J.W. Gray, F. Baehner, C.J. Park, and M.J. Bissell. 2006. Beta1 integrin inhibitory antibody induces apoptosis of breast cancer cells, inhibits growth, and distinguishes malignant from normal phenotype in three dimensional cultures and in vivo. *Cancer Res.* 66:1526–1535.

Pearson, G., F. Robinson, T. Beers Gibson, B.E. Xu, M. Karandikar, K. Berman, and M.H. Cobb. 2001. Mitogen-activated protein (MAP) kinase pathways: regulation and physiological functions. *Endocr. Rev.* 22:153–183.

Porter, D., J. Lahti-Domenici, A. Keshaviah, Y.K. Bae, P. Argani, J. Marks, A. Richardson, A. Cooper, R. Strausberg, G.J. Riggins, et al. 2003. Molecular markers in ductal carcinoma in situ of the breast. *Mol. Cancer Res.* 1:362–375.

Ridley, A.J., and A. Hall. 1992. The small GTP-binding protein rho regulates the assembly of focal adhesions and actin stress fibers in response to growth factors. *Cell*. 70:389–399.

Sahai, E., and C.J. Marshall. 2002. ROCK and Dia have opposing effects on adherens junctions downstream of Rho. *Nat. Cell Biol.* 4:408–415.

Sahai, E., and C.J. Marshall. 2003. Differing modes of tumour cell invasion have distinct requirements for Rho/ROCK signalling and extracellular proteolysis. *Nat. Cell Biol.* 5:711–719.

Schmeichel, K.L., and M.J. Bissell. 2003. Modeling tissue-specific signaling and organ function in three dimensions. *J. Cell Sci.* 116:2377–2388.

Schneider, I.C., and J.M. Haugh. 2006. Mechanisms of gradient sensing and chemotaxis: conserved pathways, diverse regulation. *Cell Cycle*. 5:1130–1134.

Schock, F., and N. Perrimon. 2002. Molecular mechanisms of epithelial morphogenesis. *Annu. Rev. Cell Dev. Biol.* 18:463–493.

Schulze, A., K. Lehmann, H.B. Jefferies, M. McMahon, and J. Downward. 2001. Analysis of the transcriptional program induced by Raf in epithelial cells. *Genes Dev.* 15:981–994.

Seton-Rogers, S.E., Y. Lu, L.M. Hines, M. Koundinya, J. LaBaer, S.K. Muthuswamy, and J.S. Brugge. 2004. Cooperation of the ErbB2 receptor and transforming growth factor beta in induction of migration and invasion in mammary epithelial cells. *Proc. Natl. Acad. Sci. USA*. 101:1257–1262.

Shakya, R., T. Watanabe, and F. Costantini. 2005. The role of GDNF/Ret signaling in ureteric bud cell fate and branching morphogenesis. *Dev. Cell*. 8:65–74.

Sivaraman, V.S., H. Wang, G.J. Nuovo, and C.C. Malbon. 1997. Hyperexpression of mitogen-activated protein kinase in human breast cancer. *J. Clin. Invest.* 99:1478–1483.

Straight, A.F., A. Cheung, J. Limouze, I. Chen, N.J. Westwood, J.R. Sellers, and T.J. Mitchison. 2003. Dissecting temporal and spatial control of cytokinesis with a myosin II Inhibitor. *Science*. 299:1743–1747.

Thiery, J.P. 2002. Epithelial-mesenchymal transitions in tumour progression. *Nat. Rev. Cancer*. 2:442–454.

Wang, W., J.B. Wyckoff, V.C. Frohlich, Y. Oleynikov, S. Huttelmaier, J. Zavadil, L. Cermak, E.P. Bottinger, R.H. Singer, J.G. White, et al. 2002. Single cell behavior in metastatic primary mammary tumors correlated with gene expression patterns revealed by molecular profiling. *Cancer Res.* 62:6278–6288.

Yu, W., X. Fang, A. Ewald, K. Wong, C.A. Hunt, Z. Werb, M.A. Matthay, and K. Mostov. 2007. Formation of cysts by alveolar type II cells in three-dimensional culture reveals a novel mechanism for epithelial morphogenesis. *Mol. Biol. Cell*. 18:1693–1700.